Modifying molecule-surface scattering by ultrashort laser pulses

Yuri Khodorkovsky,[1] J. R. Manson,[2] and Ilya Sh. Averbukh[1]

[1]*Department of Chemical Physics, The Weizmann Institute of Science, Rehovot 76100, Israel*
[2]*Department of Physics and Astronomy, Clemson University, Clemson, South Carolina 29634, USA*

In recent years it has become possible to align molecules in free space using ultrashort laser pulses. Here we explore two schemes for controlling molecule-surface scattering processes and which are based on laser-induced molecular alignment. In the first scheme, a single ultrashort nonresonant laser pulse is applied to a molecular beam hitting the surface. This pulse modifies the angular distribution of the incident molecules and causes the scattered molecules to rotate with a preferred sense of rotation (clockwise or counterclockwise). In the second scheme, two properly delayed laser pulses are applied to a molecular beam composed of two chemically close molecular species (isotopes, or nuclear-spin isomers). As the result of the double-pulse excitation, these species are selectively scattered to different angles after the collision with the surface. These effects may provide new means for the analysis and separation of molecular mixtures.

PACS number(s): 34.50.Rk, 37.10.Vz, 34.35.+a, 68.49.Df

I. INTRODUCTION

Laser control of molecular rotation, alignment, and orientation has received significant attention in recent years (for a review, see, e.g., [1,2]). Interest in the field has increased, mainly due to the improved capabilities to manipulate the characteristics of the laser pulses (such as time duration and temporal shape), which in turn lead to potential applications offered by controlling the angular distribution of molecules. Since the typical rotational time scale is "long" (~ 10 ps) compared to the typical short-pulse duration (~ 50 fs), effective rotational control and manipulation are in reach. During the last decade, coherent rotational dynamics of pulse-excited molecules was studied [3,4], and multiple-pulse sequences giving rise to enhanced alignment were suggested [5–7] and realized experimentally [8–11]. Further manipulations, such as optical molecular centrifuge and alignment-dependent strong-field ionization of molecules, were demonstrated [12,13]. Selective rotational excitation in bimolecular mixtures was suggested and demonstrated in the mixtures of molecular isotopes [14] and molecular spin isomers [15,16]. These new methods for manipulation of molecular rotation can also be used to modify the motion of molecules in inhomogeneous fields, such as focused laser beams [17–19] or static electric [20] and magnetic [21] fields.

A molecule near a solid surface can be also considered as a particle in a complicated inhomogeneous field. Although the potential energy of a molecule near a solid surface is quite complicated in all its details, there are cases when simple potential models can be used. We treat below the molecule as a rigid rotor [22], while the surface is considered flat and is described by a hard-cube model [23,24]. This model was used and gave qualitatively correct results for N_2 or NO molecules incident with thermal velocities on close-packed surfaces, such as Ag(111) (see Ref. [25] and references therein).

For simplicity, the current paper focuses on scattering from smooth surfaces, such as Ag(111). However, our treatment may be generalized to include the effects of surface corrugation by using more elaborate models such as the "washboard model" [26].

Modification of the molecule-surface scattering and molecule-surface reactions by external fields of different nature is a long-standing research problem. In particular, the effect of molecular orientation by a static electric hexapole field on the scattering process was investigated in detail [27]. Laser control of the gas-surface scattering was achieved using multiphoton ionization of the impinging molecules by long laser pulses of variable polarization [28], and the possibility of controlling molecular adsorption on solid surfaces using ultrashort laser pulses was discussed [29].

In this paper, we investigate the prospects of modifying and controlling the process of molecular scattering from solid surfaces by using ultrashort laser pulses that align molecules before they hit the surface.

The paper is organized as follows: The molecule-surface collision model is presented in Sec. II. Next, in Sec. III, the model for the interaction of a molecule with an ultrashort laser pulse is briefly explained. Next, we suggest two schemes for laser control of the molecular scattering process. In the first one, explained in Sec. IV, a single laser pulse is applied to a molecular beam in order to cause the molecules to rotate with a chosen sense of rotation (clockwise or counterclockwise) after scattering from the surface. In the second suggested scheme, explained in Sec. V, two properly delayed laser pulses are applied to a molecular beam composed of two chemically close molecular species (isotopes or nuclear spin isomers). As a result of the double-pulse excitation, the subspecular scattering angles become enriched in one of these species after the scattering from the surface. In Sec. VI we summarize and conclude.

II. MOLECULE-SURFACE SCATTERING MODEL

In this paper, we use a model in which the molecule is treated as a rigid dumbbell [24]. This dumbbell collides with a flat frictionless hard cube, which represents one of the surface atoms [23]. We assume that the cube has some velocity that is distributed according to the surface temperature. This hard-cube model provides a simple way of adding surface phonons to the molecule-surface collision process. For the sake

of simplicity, we also assume that the cube is much heavier than the molecule, so that its velocity does not change as a result of the collision. In this case, by moving to the frame attached to the cube, one reduces the problem to the molecular collision with a hard motionless wall. In the moving coordinate system, the total molecular energy (translational + rotational) is conserved, but it can be redistributed between these two parts as a result of the collision.

What about the translational linear momentum of the molecule in the moving coordinate system? The component perpendicular to the surface is not conserved, because the surface exerts forces on the molecule in this direction during the collision. On the other hand, there are no forces applied in the direction *parallel* to the frictionless surface, and therefore the linear momentum parallel to the surface is conserved. This is the reason why we can simplify the problem and consider a colliding molecule that has only a translational velocity component perpendicular to the surface. Notice that this cannot be done if the surface is corrugated.

Using energy and angular momentum conservation laws (as explained below), we find analytic expressions for the translational and the rotational velocities of the dumbbell molecule after the collision. These velocities depend on the velocities before the collision and on the angle between the dumbbell and the surface of the cube at the moment of collision. Finally, we transform the velocities back to the laboratory coordinate frame.

In the next subsections, we treat a simple case of a homonuclear molecule rotating in a plane and colliding with a hard heavy cube. Next, we extend the treatment to a three-dimensional rotation of a heteronuclear molecule. In the last subsection, we consider the effects of surface cube vibration on the collision.

A. Two-dimensional collision of homonuclear diatomic molecule

We treat a homonuclear diatomic molecule as a massless stick of length r_e, with two atoms, each of mass m, attached to its ends. To describe the molecular motion, we define the Z axis perpendicular to the surface, see Fig. 1. The angle between the molecular axis and the Z axis is θ, and it belongs to the range of $[0, 2\pi]$. The translational velocity of the center of mass is denoted by V, which is defined as positive if the molecule moves upward in Fig. 1. The linear rotational velocity is denoted by v, and is equal to $r_e\omega/2$, where ω is the angular
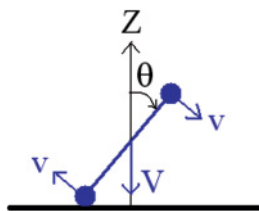

FIG. 1. (Color online) A homonuclear diatomic molecule hitting a hard flat surface. This is a two-dimensional model, where the molecule rotates only in the plane of the figure. The translational velocity of the center of mass is V, the rotational velocity of each one of the atoms, in the coordinate system moving with the center of mass, is v, and the angle between the surface normal (the Z axis) and the molecular axis is θ.

velocity of the molecular rotation. The velocity v is defined as positive if the rotation is clockwise. The velocities V and v are defined in the coordinate system moving with the velocity of the surface cube.

1. Energy conservation

The total energy conservation for the molecule is

$$\tfrac{1}{2}(2m)V_i^2 + \tfrac{1}{2}I\omega_i^2 = \tfrac{1}{2}(2m)V_f^2 + \tfrac{1}{2}I\omega_f^2, \tag{1}$$

where $I = mr_e^2/2$ is the moment of inertia, and the subscripts i and f denote the velocities before and after the collision, respectively. Simplifying the above expression we obtain:

$$V_i^2 + v_i^2 = V_f^2 + v_f^2, \tag{2}$$

or

$$(V_i - V_f)(V_i + V_f) = (v_f - v_i)(v_f + v_i). \tag{3}$$

2. Angular momentum conservation

The angular momentum of this system of two particles depends on the choice of coordinate system. We choose it such that, at the moment of collision, the origin is at the position of the colliding atom. Thus, the other atom is the only one contributing to the angular momentum of the system. Moreover, the torque exerted by the wall is zero for this choice of coordinate system. Therefore, *for this choice of coordinate system*, angular momentum is conserved during the collision. Adding velocities V and v, as defined in Fig. 1, and assuming θ is between 0 and $\pi/2$, we equate the magnitude of the angular momentum before and after the collision:

$$mr_e(v_i - V_i\sin\theta) = mr_e(v_f - V_f\sin\theta), \tag{4}$$

or

$$(V_i - V_f)\sin\theta = v_i - v_f. \tag{5}$$

Dividing (3) by (5) and using the result together with Eq. (5), we obtain the expressions for V_f and v_f:

$$\begin{aligned} V_f &= \frac{-V_i\cos^2\theta - 2v_i\sin\theta}{1 + \sin^2\theta}, \\ v_f &= \frac{v_i\cos^2\theta - 2V_i\sin\theta}{1 + \sin^2\theta}. \end{aligned} \tag{6}$$

These equations should give the same results for $\theta \to \theta + \pi$ because of the symmetry of the molecule. Because the sine function changes sign under this transformation, the correct equations for θ in the first or the third quadrant are

$$\begin{aligned} V_f &= \frac{-V_i\cos^2\theta - 2v_i|\sin\theta|}{1 + \sin^2\theta}, \\ v_f &= \frac{v_i\cos^2\theta - 2V_i|\sin\theta|}{1 + \sin^2\theta} \end{aligned} \tag{7}$$

for $0 \leqslant \theta < \pi/2$ and $\pi \leqslant \theta < 3\pi/2$.

For the angle θ in the second or fourth quadrant, the transformation $\theta \rightarrow \pi - \theta$ should be done. This is equivalent to changing v_i and v_f to $-v_i$ and $-v_f$. Finally, we obtain

$$V_f = \frac{-V_i \cos^2 \theta + 2 v_i |\sin \theta|}{1 + \sin^2 \theta},$$
$$v_f = \frac{v_i \cos^2 \theta + 2 V_i |\sin \theta|}{1 + \sin^2 \theta} \tag{8}$$

for $\pi/2 < \theta \leqslant \pi$ and $3\pi/2 < \theta \leqslant 2\pi$.

Notice that V_i is always negative and that v_f is positive (negative) for a clockwise (counterclockwise) rotation, respectively.

The angles $\theta = \pi/2$ or $3\pi/2$ are unique and are excluded from the equations above. The reason is that the treatment above is incorrect for this angle of incidence, because both atoms hit the surface at the same time, and the law of conservation of angular momentum, as applied above, cannot be applied in this specific case. However, these angles of incidence can be treated as limiting cases of a double collision, and treating them provides no particular problem, as explained below.

3. Time evolution

The above analytical expressions for translational and rotational velocities describe a *single* collision of the molecule with the surface. However, *additional collisions* may occur as well. This scenario is most evident for molecules hitting the surface at an angle close to $\pi/2$. In the case of the additional collisions, Eqs. (7) and (8) should be applied again.

Instead of finding complicated conditions for multiple collisions, we turn to a simple numerical simulation. The equations of motion for the molecule, starting at some Z_0 and θ_0 with velocities V_i and v_i, before the first collision, are simple:

$$Z(t) = Z_0 + V_i t, \tag{9}$$

and

$$\theta(t) = \theta_0 + \omega_0 t = \theta_0 + \frac{2}{r_e} v_i t \bmod (2\pi). \tag{10}$$

The collision occurs when the distance between the face of the cube and the center of mass of the molecule is equal to $0.5 r_e |\cos \theta(t)|$. At this moment in time, the velocities are transformed according to (7) or (8), and the evolution continues according to (9) and (10), using the new values of Z_0, V_i, θ_0, and v_i. We assume here that the collision lasts for a very short period of time, such that, during the collision, the values of Z and θ are practically constant.

B. Extension to three-dimensional collision of heteronuclear diatomic molecule

We describe the heteronuclear molecule as composed of two different atoms of masses m_1 and m_2, where $m_1 > m_2$. The atoms are connected by a massless rod of length r_e, as shown in Fig. 2(a). The center of mass of the molecule is closer to the heavy atom and is at a distance of $r_e/(\mu + 1)$ from it according to the definition of the center of mass. Here μ was defined as m_1/m_2. The distance between the center of mass and the light atom is, accordingly, $r_e \mu/(\mu + 1)$.
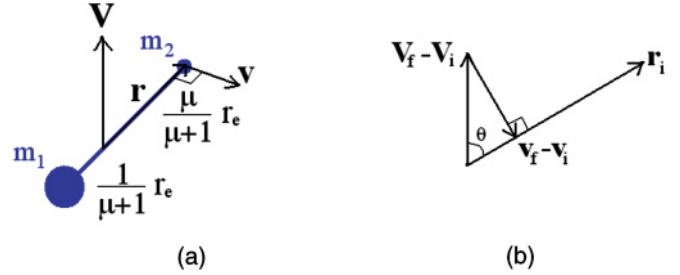

FIG. 2. (Color online) (a) Heteronuclear diatomic molecule composed of atoms of masses m_1 and m_2 (where $m_1 > m_2$) connected by a massless rod of length r_e. The translational velocity of the molecular center of mass is **V**, the molecular orientation in space is represented by the vector **r**, and the corresponding rotational velocity of the light atom is **v**. (b) Vector diagram corresponding to Eq. (A3), where the molecular orientation vector at the moment of collision is denoted by $\mathbf{r}_i$.

The molecule is characterized by the center-of-mass coordinate Z and the direction of the molecular axis, which is described by a vector $\mathbf{r} = \frac{\mu}{\mu+1} r_e (x,y,z)$, where (x,y,z) is a unit vector. This vector points from the molecular center of mass to the light atom of mass m_2 [see Fig. 2(a)]. The corresponding velocity is given by $\mathbf{v} = d\mathbf{r}/dt$. Therefore, the linear velocity (in the center-of-mass coordinate system) of the light atom is **v** and that of the heavy atom is $-\mathbf{v}/\mu$.

After a derivation similar to the one for the two-dimensional (2D) rotation presented above, we obtain expressions connecting the velocities before the collision, $\mathbf{V}_i$ and $\mathbf{v}_i$, to the velocities after the collision, $\mathbf{V}_f$ and $\mathbf{v}_f$ [see Eqs. (A8), (A4), (A10), and (A11)]. The molecule, at the moment of collision, is oriented at $\mathbf{r}_i$ [see Fig. 2(b)]. The details of the derivation are given in the appendix at the end of the paper.

For a free-rotating heteronuclear molecule, the end of the vector **r** traces a circle with radius equal to $\frac{\mu}{\mu+1} r_e$. The orientation in space of the circle is defined by the initial orientation $\mathbf{r}_0$ and the initial velocity $\mathbf{v}_0$. The orientation of the molecule at time t is thus given by

$$\mathbf{r}(t) = \mathbf{r_0} \cos(v_0 t) + \frac{\mu}{\mu+1} r_e \frac{\mathbf{v_0}}{v_0} \sin(v_0 t), \tag{11}$$

where $v_0 = |\mathbf{v_0}|$. Taking the derivative, the velocity is

$$\mathbf{v}(t) = -v_0 \mathbf{r_0} \sin(v_0 t) + \frac{\mu}{\mu+1} r_e \mathbf{v_0} \cos(v_0 t). \tag{12}$$

Finally, we emphasize that the molecular collision with the surface of the cube occurs when the molecule is oriented with $z_i > 0$ and the distance between the face of the cube and the center of mass of the molecule is equal to $r_e |\cos \theta|/(\mu + 1)$ *or* when the molecule is oriented with $z_i < 0$ and the distance between the face of the cube and the center of mass of the molecule is equal to $r_e |\cos \theta| \mu/(\mu + 1)$.

C. Vibration of surface atoms—simple inclusion of phonons

The hard-cube model [23,24,30] provides a simple way to include surface-atom vibrations into the collision process. The collision of a molecule with a hard wall of infinite mass is replaced by a collision with a hard cube of finite, but large, mass M moving with velocity U. For simplicity, we assume

that the cube oscillates in a hard box of a finite size. In the model, the cube oscillates in the direction perpendicular to the surface plane. The reason is that, for a flat and frictionless cube, only the vertical velocity component can transfer energy to the impinging molecule. The cube moves with a constant speed, while the velocity reverses its direction at the ends of the hard box. The one-dimensional velocity of the hard cube is random and is distributed according to a Boltzmann distribution:

$$f(U) = \sqrt{\frac{M}{2\pi k_B T_{\text{surf}}}} \exp\left(-\frac{MU^2}{2k_B T_{\text{surf}}}\right), \qquad (13)$$

where T_{surf} is the temperature of the solid surface and k_B is the Boltzmann constant. When treating the collision process, we assume that the mass of the surface atom is much larger than the mass of the molecule (i.e., $M \gg m_1 + m_2$) so that the collision does not change significantly the velocity of the hard cube. Only the velocities of the molecule change, and its total energy in the laboratory coordinate frame may increase or decrease.

The previous treatment of the collision in the coordinate frame moving with the cube is now easily incorporated into the model. The collision condition (for a homonuclear molecule) can be expressed as

$$Z(t) - Z_M(t) = \tfrac{1}{2} r_e |\cos\theta(t)|, \qquad (14)$$

where $Z_M(t)$ is the time-dependent position of the surface of the hard cube. According to the assumptions above, $Z_M(t)$ is a simple "zigzag" function (triangle wave). The amplitude A of the function $Z_M(t)$ is taken as the representative amplitude of a one-dimensional harmonic oscillator with an average energy of $k_B T_{\text{surf}}$ and is given by $A = \sqrt{(k_B T_{\text{surf}})/(M\omega^2)}$. Here, ω corresponds to the vibrational angular frequency of a single surface atom and is approximately equal to 10^{13} Hz for the case of the Ag(111) surface [31]. The oscillation frequency of the "zigzag" function is determined by the speed $|U|$ of the cube and by the amplitude A.

The translational velocity of the molecule is transformed before the collision according to $V_i \rightarrow V_i - U_{\text{col}}$, where U_{col} is the velocity of the hard cube at the moment of collision. This is a usual Galilean transformation to the coordinate frame moving with the hard cube. Similarly, after the collision, the translational velocity of the molecule is transformed back by $V_f \rightarrow V_f + U_{\text{col}}$. The rotational velocity remains unchanged under this Galilean transformation.

III. INTERACTION OF MOLECULE WITH ULTRASHORT LASER PULSE

Here, we briefly summarize the results of the classical model describing the interaction of the diatomic rigid molecule with a nonresonant ultrashort laser pulse in the impulsive approximation. A more detailed description may be found in Ref. [32].

The potential energy of the laser pulse interacting with the induced molecular dipole is given by

$$V(\theta,\varphi,t) = -\tfrac{1}{4}\mathcal{E}^2(t)(\Delta\alpha\cos^2\beta + \alpha_\perp), \qquad (15)$$

where $\Delta\alpha = \alpha_\parallel - \alpha_\perp$ is the difference between the polarizability along the molecular axis and the polarizability

perpendicular to it, $\mathcal{E}(t)$ is the envelope of the electric field of the *linearly polarized* laser pulse, and $\beta = \beta(\theta,\varphi)$ is the angle between the molecular axis and the direction of polarization of the pulse. Here θ,φ are the polar and the azimuthal angles, respectively, characterizing the orientation of the molecular axis. We assume that the pulse duration is very short compared to the rotational period, so that the pulse can be described in the impulsive (δ-kick) approximation. We define the dimensionless interaction strength P, which characterizes the pulse, as

$$P = \frac{\Delta\alpha}{4\hbar} \int_{-\infty}^{\infty} \mathcal{E}^2(t)dt. \qquad (16)$$

We consider the action of a pulse linearly polarized along some arbitrary unit vector **p** and determine the vector of the resulting velocity change $\Delta\mathbf{v}$ for a molecule oriented along some direction $\mathbf{r_0}$. The norm $|\Delta\mathbf{v}|$ can be found by integrating Newton's equations of motion for a pulse polarized along the z axis. It is equal to $\frac{\hbar}{I}|P\sin 2\beta_0|$, where β_0 is the angle between the polarization direction of the pulse **p** and the orientation direction of the molecule $\mathbf{r_0}$, and I is the moment of inertia of the molecule. Notice that $\Delta\mathbf{v}$ is always perpendicular to $\mathbf{r_0}$. Also, $\Delta\mathbf{v}$ is directed parallel or antiparallel to the vector component of **p** perpendicular to $\mathbf{r_0}$, which is equal to $\mathbf{p} - \frac{\mu+1}{\mu r_e}\cos\beta_0\mathbf{r_0}$. As a result, we arrive at

$$\Delta\mathbf{v} = \frac{2\hbar P}{I}\cos\beta_0\left(\frac{\mu}{\mu+1}r_e\mathbf{p} - (\cos\beta_0)\mathbf{r_0}\right). \qquad (17)$$

IV. "MOLECULAR PROPELLER" INDUCED BY LASER ALIGNMENT AND COLLISION WITH SURFACE

In this section we explore a way of inducing unidirectional molecular rotation by a single laser pulse and a single surface-scattering event. The idea is inspired by a recent scheme that was proposed in [33,34] and realized experimentally in [35]. In these papers, two time-delayed and cross-polarized laser pulses were used to induce molecular rotation in a preferred sense. Here we achieve a similar goal by replacing the second laser pulse by the process of molecular scattering from a solid surface.

Before presenting our scheme, we summarize shortly the purely optical scheme described in [32–35]. We start with a gas of diatomic molecules in free space. The first ultrashort laser pulse, linearly polarized along the z axis, induces a coherent molecular rotation that continues after the end of the pulse. The molecules rotate under field-free conditions until they reach an aligned state in which the molecular axis with the highest polarizability is confined to a narrow cone around the polarization direction of the first pulse. The second short laser pulse is applied at the moment of best alignment and at an angle with respect to the first pulse. As a result, the aligned molecular ensemble experiences a torque causing molecular rotation in the plane defined by the two polarization vectors. The rotational velocity delivered to a linear molecule is maximal when the laser pulse is polarized at 45° with respect to the molecular axis of the highest polarizability, as can be seen from Eq. (17). This defines the optimal angle between the laser pulses. The direction of the excited rotation (clockwise or counterclockwise) is determined by the sign of

the relative angle ($\pm 45°$) between the first and the second pulse in the polarization plane. This double-pulse scheme was termed a "molecular propeller," because it resembles the action needed to ignite a rotation of a plane propeller.

In the current scheme, we start from a monoenergetic molecular beam of diatomic molecules flying toward a flat surface at the incidence angle of 45°. For simplicity, all the molecules have the same velocity vector. Before hitting the surface, the molecules are aligned by a laser pulse polarized at $+45°$ to the surface. When colliding with the surface, the aligned molecules receive a "kick" from it and scatter with rotation in a specific direction. Changing the polarization angle of the laser with respect to the surface to $-45°$, the sense of rotation of the scattered molecules can be inverted. It is important to emphasize that it is not required that the molecules aligned by the laser pulse hit the surface at some specific time after the aligning pulse. Differently, in the double-pulse scheme from the previous paragraph, the time delay between the two pulses is important.

In order to properly analyze the scattering of a molecular beam, we need to account for the spatial spread of the molecules inside the beam. For typical experimental conditions, this spread is of the order of 1 mm in the direction transverse to the propagation direction of the molecular beam. This spread (which we denote by b) is determined by the diameter of the collimating aperture in the experimental system [36]. A similar spread can be observed in the direction longitudinal to the direction of the beam propagation, if one uses the pulsed-molecular-beam technique [37].

The typical angle uncertainty due to the transverse spatial spread of the molecular beam hitting the surface is given by the ratio of the above spread and the distance between the surface and the detector, denoted by R. If this angle, equal to b/R, is negligible compared with the angular spread of the scattered molecules, then the transverse spatial spread can be neglected in the simulation. For a transverse spatial spread of the molecular beam of about 1 mm and for a distance between the surface and detector of 10 cm, the angle uncertainty is about 0.01 rad or 0.6°. This number is negligible compared with the angular spread we obtain in our simulation results (see, e.g., Fig. 7). Therefore, in our simulations we can safely neglect the spread of the molecular beam in the transverse direction and concentrate on the longitudinal spread.

After the molecules are "kicked" by the laser pulse, they start rotating in a concerted way, while continuing to approach the surface. The angular distribution of the "kicked" molecules, after averaging over a long time period, is elongated along the pulse polarization direction as was shown in [32] and as is depicted schematically in Fig. 3 by the cigar-shaped distribution. The result of this time averaging is the same as that of the averaging along the distance parallel to the direction of molecular propagation, because time is related to distance by $Z = V_0 t / \sqrt{2}$ for all the molecules. From the above we conclude that, *on average,* the molecules approaching the surface are aligned along the polarization direction of the ultrashort laser pulse. We stress that this is true classically as well as quantum mechanically. If the molecules are aligned at 45° with respect to the surface, they have a preferred orientation while colliding with the surface. These molecules receive a "kick" from the surface, which leads to the preferred
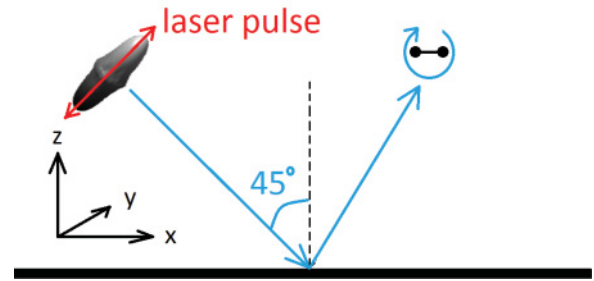

FIG. 3. (Color online) A molecular beam impinges on a hard-wall surface at an angle of 45°. Before hitting the surface, the molecules are "kicked" by an ultrashort laser pulse polarized as shown by the double-headed (red) arrow. This pulse generates the *time-averaged* angular distribution of the molecular orientation in the form of the "cigar," as shown. These aligned molecules are preferentially rotating clockwise after hitting the surface.

sense of rotation; for example, a clockwise rotation as in Fig. 3. If we plot the distribution of the components of angular momentum of the scattered molecules, we expect to see an asymmetry that is correlated with the polarization direction of the exciting pulse.

In the following, we show the results of a Monte Carlo simulation, according to the above scheme, calculated using 5×10^4 N_2 molecules hitting a flat hard-cube surface with an angle of incidence of 45°. The molecules move with an initial velocity of $V_0 = 350$ m/s and with a rotational temperature of $T_{rot} = 1$ K, which is typical for molecular beam experiments. The molecular velocities in this and the next section are determined according to a Boltzmann distribution. The molecules receive a kick with a strength of $P = 10$ from an ultrashort laser pulse, before hitting the surface. We choose the surface to be Ag(111), with the appropriate mass M of the representative hard cube, and the surface temperature is taken to be $T_{surf} = 300$ K. We choose the polarization direction of the exciting pulse to be $\mathbf{p} = (1,0,1)/\sqrt{2}$ (i.e., at 45° to the surface in the xz plane), as shown in Fig. 3.

Figure 4 shows the distribution functions of the angular momentum components J_x, J_y, and J_z after the scattering. On the left set of panels, distribution functions for molecules that were *not* excited by the laser pulse are shown. The distribution functions on the left set of panels are, in general, narrow, because of the initial low rotational temperature of the molecules. The small background seen for the J_x and J_y distribution (absent at J_z) appears because of the forces in the z direction exerted by the surface on the molecules. These forces in the z direction produce torques that change the angular momenta in the x and the y but not in the z direction. In the right set of panels, distribution functions for molecules that *were* excited by the laser pulse are shown for comparison. We see that the distributions of J_x and J_z are symmetric around zero, as expected from the symmetry of the pulse. However, most of the molecules are scattered with positive J_y. In addition, the distribution functions on the right set of panels are wider than on the left set because of the angular momentum transferred to the molecules by the laser pulse. The maximum value of J_y in the right middle panel is around $5\hbar$ (notice that $\hbar$ appears only for the purpose of showing the classical results in convenient units). This maximum coincides with the
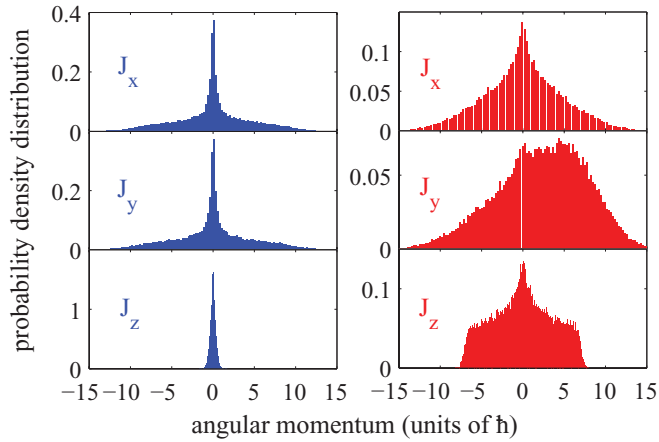
FIG. 4. (Color online) Distribution of angular momentum components J_x, J_y, and J_z of the molecules scattered from a hard-cube surface are plotted in the panels. On the right set of panels, the molecules are manipulated with an ultrashort laser pulse before hitting the surface, as shown in Fig. 3, while on the left set of panels there is no laser excitation. As expected, the distribution of J_y for laser-excited molecules (on the right set of panels) is asymmetric, and there are more molecules with a positive J_y. The average value of J_y is $\langle J_y \rangle = 2.3\hbar$. The calculation is done with the hard-cube model for nitrogen molecules (atomic mass of 28 amu) incident with translational velocity of 350 m/s and rotational temperature of $T_{rot} = 1$ K. The laser pulse strength is $P = 10$, and the polarization angle is $\gamma = 45°$. The surface is composed of silver atoms at room temperature ($M = 108$ amu and $T_{surf} = 300$ K). In this and all other figures the results of a Monte Carlo simulation of 5×10^4 molecules are shown.

value of $5.6\hbar$, which may be estimated by using Eq. (7) for v_f and the appropriate molecular constants m and r_e. This estimation considers a representative nonrotating molecule oriented at $\theta = \pi/4$ and impinging on the surface with an incident velocity of $V_i = 350/\sqrt{2}$ m/s.

Switching the polarization direction to $\mathbf{p} = (-1, 0, 1)/\sqrt{2}$ inverts the J_y distribution of the scattered molecules, making it peak at negative values of J_y. In Fig. 5 we plot by the dashed (green) line the average induced y component of the angular momentum as a function of the angle of the linear polarization direction of the pulse in the xz plane. We denote this angle by γ, so that a pulse polarized along the z axis corresponds to $\gamma = 0$. It is seen, as expected, that the largest induced $\langle J_y \rangle$ is obtained for a polarization angle close to $45°$. Switching the polarization direction to $-45°$ results in the largest induced $|\langle J_y \rangle|$ with an opposite sign.

V. LASER-CONTROLLED SURFACE SCATTERING AND SEPARATION OF MOLECULAR MIXTURES

In this section, we show that, in principle, one may use laser-controlled surface scattering for separating molecular beams consisting of several molecular species into individual components. The scheme seems to be applicable to different types of molecular species, such as isotopes or nuclear-spin isomers. It takes advantage of the fact that rotationally excited and unexcited molecules have different scattering angle distributions after collision with the surface.
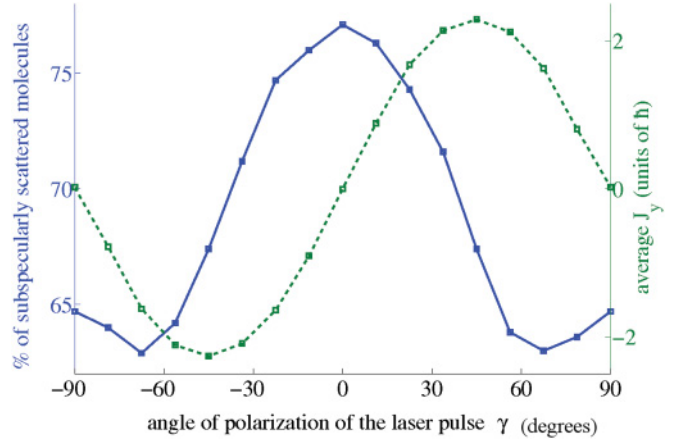

FIG. 5. (Color online) Percentage of the laser-excited molecules scattered to the subspecular angles as a function of the polarization angle of the pulse γ (solid blue line). The dashed green line represents the average induced angular momentum component $\langle J_y \rangle$ as a function of γ. The parameters are the same as in Fig. 4. The squares represent the results of the simulations, and the lines are shown only to guide the eye.

As an example, we consider a molecular beam composed of a mixture of two nitrogen species. They can be two molecular isotopes, such as $^{14}N_2$ and $^{15}N_2$, or two nuclear-spin isomers, such as ortho and para isomers of $^{15}N_2$.

It was shown in the past, both theoretically and experimentally, that two properly delayed ultrashort laser pulses may selectively align a preferred component of such a mixture, while leaving the other component practically unexcited (see [14–16]).

In order to explain this manipulation, a quantum description of the kicked molecules should be used. After the molecules are kicked by a single laser pulse, they are transiently aligned, and shortly thereafter become randomly oriented again. However, because the quantum energy levels of the rotor are discrete, and because of the symmetry of a linear molecule, the molecular alignment reappears periodically due to the phenomenon of quantum revival of the rotational wave packet. Generally, the dynamics of the rotational wave function repeats itself after a fixed time period called the *revival time*, which is proportional to the moment of inertia of the molecule [38,39].

It was shown in [14] that molecules aligned by the first laser pulse may become even more significantly aligned if a second laser pulse is applied to them, which is delayed by an integer multiple of the revival time. However, if the time delay between the two pulses is close to a half-integer multiple of the revival time, the rotational energy given to the molecules by the first pulse is taken away by the second pulse, and the molecules practically return to the unexcited isotropic state they were in before the first pulse.

Consider now a mixture of two isotopes as mentioned above. Because of the mass difference of the isotopes, they have different revival times. After this mixture is kicked by the first pulse, it is possible to find delay times such that one of the isotopes evolves for an integer number of revival periods, while the second one completes a half-integer number of its own periods. If the second pulse is applied at one of these moments, then the first isotope will experience enhanced rotational
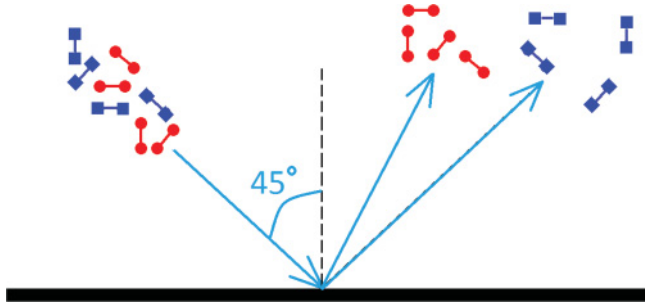
FIG. 6. (Color online) A mixture of two molecular species is manipulated by two properly delayed ultrashort laser pulses before hitting the surface. The species represented by dumbbells with square ends (blue) are rotationally cold (their rotation is deexcited by the second laser pulse). The species represented by dumbbells with circular ends (red) are rotationally hot (their rotation was further enhanced by the second laser pulse). After hitting the surface, the "blue" species are mostly scattered specularly and toward angles larger than the specular angle. On the other hand, the "red" species mostly transfer their rotational energy to translational energy, and are scattered to angles smaller than the specular angle.

alignment, while the second one will become isotropic and rotationally deexcited.

A similar double-pulse approach can be used for selective alignment in a mixture of nuclear-spin isomers of $^{15}N_2$, as explained in Ref. [16]. In this case, both isomers have the same mass and, therefore, the same revival time. However, kicking the molecules with a second pulse delayed by a time close to an $n + 1/4$ (or a $n + 3/4$) multiple of the revival time (where n is a positive integer) provides further rotational excitation of one of the isomers, while deexciting the other isomer. The reason for this effect is the correlation between the molecular rotational and nuclear spin degrees of freedom, which is imposed by the Pauli principle (for details, see [16]).

Assume now that such a selectively excited molecular beam hits a solid surface, as shown schematically in Fig. 6. For a moment, we also assume that the surface is not vibrating (i.e., stays frozen at zero temperature). According to Eq. (1), the rotationally hot (aligned) molecular species, represented by dumbbells with circular ends (red) in Fig. 6, have a high probability of transferring their rotational energy to translational energy via the collision. As a result, the perpendicular component of the molecular velocity after the collision is larger than that before the scattering (the parallel velocity component remains the same). In other words, these molecules have a high probability to be scattered to angles smaller than the specular angle (i.e., to "subspecular" angles). The second species, which are rotationally cold (and isotropically oriented) and are represented by dumbbells with square ends (blue) in Fig. 6, have a high probability to transfer their translational energy to rotational energy, and they are mainly scattered to angles larger than the specular angle. As a result of the scattering process, the molecular mixture that arrives to the region of subspecular angles is highly enriched with the "circular atom" (red) species. At finite temperature of the surface, the effect is somehow reduced. The reason is that even a nonrotating molecule can acquire translational energy from a vibrating surface atom moving toward it and scatter to subspecular angles. However,
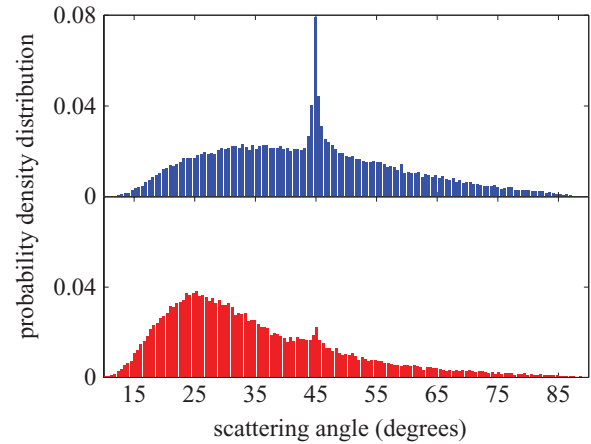

FIG. 7. (Color online) Scattering angle distribution of the "square atom" (blue) species at the top and the "circular atom" (red) species at the bottom, according to the scheme of Fig. 6. The calculation is done using the hard-cube model for nitrogen molecules incident on the surface with translational velocity of 350 m/s and rotational temperature of $T_{rot} = 1$ K. The distribution at the top panel is for molecules that are not excited by the laser, in order to represent the species that are deexcited by the second laser pulse. The distribution at the bottom panel is for molecules that are excited by a laser pulse with $P = 10$ and $\gamma = 0$ to represent the species that are excited twice by a laser pulse with $P = 5$. In the upper panel of the figure, only 52% of the molecules are scattered to subspecular angles, while in the lower panel, 77% are scattered to these angles. This means that almost 50% enrichment is achieved for the selectively excited isotope. The surface cube parameters correspond to silver atoms at room temperature ($M = 108$ amu and $T_{surf} = 300$ K).

for a sufficiently strong laser pulse, a sizable effect is expected even for surfaces at room temperature.

To estimate the magnitude of the effect for typical experimental conditions, we consider scattering of a beam consisting of a 1:1 mixture of the two nitrogen species discussed above. The beam has an initial translational velocity of 350 m/s, a rotational temperature of $T_{rot} = 1$ K, and it propagates at 45° with respect to the surface. The surface consists of silver atoms, and the surface temperature is $T_{surf} = 300$ K. Before hitting the surface, the molecules are excited by a pair of laser pulses of $P = 5$ that are polarized along $\mathbf{p} = (0,0,1)$ direction. The timing between the pulses is chosen such that one of the species remains rotationally unexcited, while the other one experiences an effective kick of $P = 10$ from the double pulse. In Fig. 7 we plot the distribution of the scattering angle for the two molecular isotopes. The upper panel of this figure corresponds to the unexcited component of the molecular beam. The lower panel corresponds to the selectively excited isotope. In both parts of the figure, the distributions are peaked around 25°–30°, in addition to the specular peak at 45°. This peak comes from the translational energy delivered to the molecules by the thermally oscillating surface atoms. It is easy to understand the appearance of the maximum around 25° by using the following simple arguments. Consider a ball with velocity v, colliding with a heavy cube moving toward it with velocity U. This ball is reflected from the cube with velocity $v + 2U$. Treating the molecule as a ball and keeping in mind that it hits the cube at angle of 45°, we arrive at a
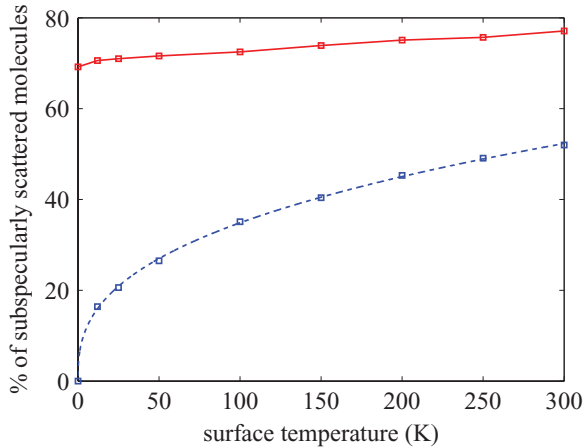
FIG. 8. (Color online) Percentage of subspecularly scattered molecules plotted as a function of surface temperature for scattering of rotationally hot molecules (solid red curve) and for rotationally cold molecules (dashed blue curve). The parameters chosen for the calculation here are the same as for Fig. 7, except for the surface temperature. The squares represent the results of the simulations and the lines are shown only to guide the eye. The dashed (blue) line is a smooth fit of a power function to the results.

scattering angle of $\arctan(\frac{v/\sqrt{2}}{v/\sqrt{2}+2U})$. Using a typical value of $\sqrt{k_B T_{\text{surf}}/M} = 150$ m/s for the velocity U, and an incident velocity v of 350 m/s, we estimate the scattering angle of $24°$, which is consistent with the distribution maxima seen in Fig. 7.

Analyzing the distribution functions of Fig. 7, we find that 77% of the rotationally hot species are scattered to the subspecular angles, while only 52% of the rotationally cold species are scattered to these angles, which means almost 50% enrichment in the selectively excited isotope. This figure is remarkable by itself; however, it becomes even more impressive at lower surface temperature. In Fig. 8 we plot the percentage of the subspecularly scattered molecules for the rotationally cold species (dashed blue line), and for the rotationally hot species (solid red line) as a function of the surface temperature. We observe that, for any temperature between zero and room temperature, there are more laser-excited molecules scattered to subspecular angles than there are unexcited molecules. The effect is enhanced dramatically for surface temperatures below 50 K, and the ratio between the two isotopes asymptotically tends to the impressive value of more than 70 at zero surface temperature! This suggests that cooling the solid surface increases the effect to a large extent.

We also explored the dependence of scattering on the laser polarization direction γ defined at the end of Sec. IV. In Fig. 5 we plot by the solid (blue) line the percentage of the rotationally hot molecules scattered toward subspecular angles as a function of the angle γ. We find that the percentage varies slightly with the polarization direction and that the maximal percentage is obtained for pulses polarized at $\gamma = 0$.

VI. CONCLUSIONS

We presented a simple classical model based on the hard-cube model to describe laser-induced control of molecule-surface scattering. Based on this model, we investigated two possible schemes for modifying the scattering process.

In the first scheme, we considered excitation of the unidirectional molecular rotation via the combined action of short laser pulses and surface collisions. As a first step, the molecules of the molecular beam are aligned by a laser pulse polarized at a given angle with respect to the surface. Then, after the surface scattering, the molecules are shown to rotate preferentially in a direction determined by the laser polarization vector and the surface normal. This orientation of the angular momentum of the scattered molecules can be detected, for example, by using resonance-enhanced multiphoton ionization (REMPI) spectroscopy [35,40]. In the second scheme, we suggest exciting a molecular beam, consisting of two molecular species, by two properly delayed laser pulses in order to provide selective rotational excitation of one of the species (similar to [14] and [16]). We have shown that these two species are then scattered differently from a solid surface, in a way that the scattered beam is enriched in one of the species, for subspecular scattering angles. This result is potentially interesting for the analysis and separation of molecular mixtures of different kinds, including isotopes and molecular nuclear-spin isomers.

APPENDIX: THREE-DIMENSIONAL SCATTERING OF HETERONUCLEAR DIATOMIC MOLECULES FROM A HARD WALL

1. Energy conservation

The conservation of the total (translational and rotational) energy before and after the collision is, similar to Eq. (1),

$$\frac{1}{2}(m_1 + m_2)V_i^2 + \frac{1}{2}\frac{m_1 m_2}{m_1 + m_2}r_e^2\omega_i^2$$
$$= \frac{1}{2}(m_1 + m_2)V_f^2 + \frac{1}{2}\frac{m_1 m_2}{m_1 + m_2}r_e^2\omega_f^2$$

or, using the quantities $\mu = m_1/m_2$ and $v = \frac{\mu}{\mu+1}r_e\omega$:

$$V_i^2 + \frac{1}{\mu}v_i^2 = V_f^2 + \frac{1}{\mu}v_f^2. \tag{A1}$$

2. Angular momentum conservation

Angular momentum conservation in the coordinate system centered at the colliding atom should be expressed now in vector form. The molecule hits the surface when oriented at some $\mathbf{r}_i = \frac{\mu}{\mu+1}r_e(x_i, y_i, z_i)$. The collision is very fast, such that the velocities change, but the orientation remains the same ($\mathbf{r}_f = \mathbf{r}_i$) over the course of the collision.

We start with the case when the molecule hits the surface with the heavier atom of mass m_1 or with $z_i > 0$. Angular momentum conservation gives, similar to Eq. (4),

$$m_2 \frac{\mu + 1}{\mu} \mathbf{r}_i \times (\mathbf{V}_i + \mathbf{v}_i) = m_2 \frac{\mu + 1}{\mu} \mathbf{r}_i \times (\mathbf{V}_f + \mathbf{v}_f), \quad \text{(A2)}$$

or

$$\mathbf{r}_i \times (\mathbf{V}_f - \mathbf{V}_i + \mathbf{v}_f - \mathbf{v}_i) = \mathbf{0}. \quad \text{(A3)}$$

It follows from the last equation that the vector in the parentheses should be parallel (or antiparallel) to $\mathbf{r}_i$. The vector $\mathbf{V}_f - \mathbf{V}_i$ is perpendicular to the surface, because we only treat the velocity component perpendicular to the surface (the hard cube is flat and frictionless). The vector $\mathbf{v}_f - \mathbf{v}_i$ should be perpendicular to $\mathbf{r}_i$, because both $\mathbf{v}_i$ and $\mathbf{v}_f$ are perpendicular to $\mathbf{r}_i$. All this leads to the vector diagram in Fig. 2(b). It follows from the diagram that

$$|\mathbf{v}_f - \mathbf{v}_i| = |V_f - V_i| \sin \theta, \quad \text{(A4)}$$

an expression similar to Eq. (5), where V_i and V_f denote the center-of-mass velocities with the appropriate sign, and $\sin^2 \theta = x_i^2 + y_i^2$ (in the three-dimensional case, the angle θ varies between 0 and π so that $\sin \theta$ is always positive). By squaring the last equation, we obtain

$$v_f^2 + v_i^2 - 2\mathbf{v}_i \cdot \mathbf{v}_f = (V_f - V_i)^2 \sin^2 \theta. \quad \text{(A5)}$$

The final velocity v_f can be substituted from Eq. (A1). The dot product can be found from the following expression:

$$(\mathbf{v}_f - \mathbf{v}_i) \cdot \mathbf{v}_i = \mathbf{v}_i \cdot \mathbf{v}_f - v_i^2 = |\mathbf{v}_f - \mathbf{v}_i| v_i \vec{e}_{v_i} \cdot \vec{e}_{v_f - v_i}, \quad \text{(A6)}$$

where $\vec{e}_{v_i}$ and $\vec{e}_{v_f - v_i}$ are the unit vectors in the direction of $\mathbf{v}_i$ and $\mathbf{v}_f - \mathbf{v}_i$, respectively. The unit vector $\vec{e}_{v_f - v_i}$ can be easily found using Fig. 2(b):

$$\vec{e}_{v_f - v_i} = -\frac{\vec{e}_z - (\vec{e}_z \cdot \mathbf{r}_i) \mathbf{r}_i}{\sqrt{1 - (\vec{e}_z \cdot \mathbf{r}_i)^2}}, \quad \text{(A7)}$$

where $\vec{e}_z$ is the unit vector in the direction perpendicular to the surface [the direction of $\mathbf{V}_f - \mathbf{V}_i$ in Fig. 2(b)].

Finally, combining Eqs. (A1), (A4), (A5), and (A6), we obtain V_f, which can be positive or negative:

$$V_f = \frac{(\sin^2 \theta - \mu) V_i - 2|v_i| \sin \theta (\vec{e}_{v_i} \cdot \vec{e}_{v_f - v_i})}{\sin^2 \theta + \mu}. \quad \text{(A8)}$$

By using Eqs. (A4), (A7), and (A8) it is easy to find $\mathbf{v}_f$ as well.

Now we analyze the case when the molecule hits the surface with the lighter atom of mass m_2, or with $z_i < 0$. Here, energy conservation is the same, but angular momentum conservation is

$$-m_1 \frac{\mu + 1}{\mu} \mathbf{r}_i \times \left(\mathbf{V}_i - \frac{1}{\mu} \mathbf{v}_i\right)$$
$$= -m_1 \frac{\mu + 1}{\mu} \mathbf{r}_i \times \left(\mathbf{V}_f - \frac{1}{\mu} \mathbf{v}_f\right). \quad \text{(A9)}$$

After a similar derivation, we find

$$V_f = \frac{(\mu \sin^2 \theta - 1) V_i - 2|v_i| \sin \theta (\vec{e}_{v_i} \cdot \vec{e}_{v_f - v_i})}{\mu \sin^2 \theta + 1}, \quad \text{(A10)}$$

and

$$|\mathbf{v}_f - \mathbf{v}_i| = \mu |V_f - V_i| \sin \theta. \quad \text{(A11)}$$

It can be easily checked that Eqs. (A8), (A4), (A10), and (A11) reduce to Eqs. (7) and (8) for $\mu = 1$ and a two-dimensional rotation.

---

[1] H. Stapelfeldt and T. Seideman, Rev. Mod. Phys. **75**, 543 (2003).

[2] T. Seideman and E. Hamilton, Adv. At. Mol. Opt. Phys. **52**, 289 (2006).

[3] J. Ortigoso, M. Rodriguez, M. Gupta, and B. Friedrich, J. Chem. Phys. **110**, 3870 (1999).

[4] F. Rosca-Pruna and M. J. J. Vrakking, Phys. Rev. Lett. **87**, 153902 (2001).

[5] I. Sh. Averbukh and R. Arvieu, Phys. Rev. Lett. **87**, 163601 (2001); M. Leibscher, I. Sh. Averbukh, and H. Rabitz, *ibid.* **90**, 213001 (2003).

[6] M. Leibscher, I. Sh. Averbukh, and H. Rabitz, Phys. Rev. A **69**, 013402 (2004).

[7] M. Renard, E. Hertz, S. Guérin, H. R. Jauslin, B. Lavorel, and O. Faucher, Phys. Rev. A **72**, 025401 (2005).

[8] C. Z. Bisgaard, M. D. Poulsen, E. Péronne, S. S. Viftrup, and H. Stapelfeldt, Phys. Rev. Lett. **92**, 173004 (2004).

[9] K. F. Lee, I. V. Litvinyuk, P. W. Dooley, M. Spanner, D. M. Villeneuve, and P. B. Corkum, J. Phys. B **37**, L43 (2004).

[10] C. Z. Bisgaard, S. S. Viftrup, and H. Stapelfeldt, Phys. Rev. A **73**, 053410 (2006).

[11] D. Pinkham and R. R. Jones, Phys. Rev. A **72**, 023418 (2005).

[12] J. Karczmarek, J. Wright, P. Corkum, and M. Ivanov, Phys. Rev. Lett. **82**, 3420 (1999).

[13] I. V. Litvinyuk, K. F. Lee, P. W. Dooley, D. M. Rayner, D. M. Villeneuve, and P. B. Corkum, Phys. Rev. Lett. **90**, 233003 (2003).

[14] Sh. Fleischer, I. Sh. Averbukh, and Y. Prior, Phys. Rev. A **74**, 041403 (2006).

[15] M. Renard, E. Hertz, B. Lavorel, and O. Faucher, Phys. Rev. A **69**, 043401 (2004).

[16] Sh. Fleischer, I. Sh. Averbukh, and Y. Prior, Phys. Rev. Lett. **99**, 093002 (2007).

[17] S. M. Purcell and P. F. Barker, Phys. Rev. Lett. **103**, 153001 (2009); Phys. Rev. A **82**, 033433 (2010).

[18] E. Gershnabel and I. Sh. Averbukh, Phys. Rev. Lett. **104**, 153001 (2010); Phys. Rev. A **82**, 033401 (2010).

[19] J. Floß, E. Gershnabel, and I. Sh. Averbukh, Phys. Rev. A **83**, 025401 (2011).

[20] E. Gershnabel and I. Sh. Averbukh, J. Chem. Phys. **134**, 054304 (2011).

[21] E. Gershnabel, M. Shapiro, and I. Sh. Averbukh (to be published).

[22] H. Ambaye and J. R. Manson, J. Chem. Phys. **125**, 084717 (2006).

[23] R. M. Logan and R. E. Stickney, J. Chem. Phys. **44**, 195 (1966).

[24] J. D. Doll, J. Chem. Phys. **59**, 1038 (1973).

[25] M. E. M. Spruit, P. J. van den Hoek, E. W. Kuipers, F. H. Geuzebroek, and A. W. Kleyn, Phys. Rev. B **39**, 3915 (1989).

[26] J. C. Tully, J. Chem. Phys. **92**, 680 (1990).

[27] E. W. Kuipers, M. G. Tenner, A. W. Kleyn, and S. Stolte, Nature (London) **334**, 420 (1988); M. G. Tenner, E. W. Kuipers, A. W. Kleyn, and S. Stolte, J. Chem. Phys. **94**, 5197 (1991).

[28] J. N. Greeley, J. S. Martin, J. R. Morris, and D. C. Jacobs, J. Chem. Phys. **102**, 4996 (1995); R. N. Zare, Science **279**, 1875 (1998).

[29] D. Shreenivas, A. Lee, N. Walter, D. Sampayo, S. Bennett, and T. Seideman, J. Phys. Chem. A **114**, 5674 (2010).

[30] F. O. Goodman, J. Phys. Chem. Solids **26**, 85 (1965).

[31] R. B. Doak, U. Harten, and J. P. Toennies, Phys. Rev. Lett. **51**, 578 (1983).

[32] Y. Khodorkovsky, K. Kitano, H. Hasegawa, Y. Ohshima, and I. Sh. Averbukh, Phys. Rev. A **83**, 023423 (2011).

[33] S. Fleischer, Y. Khodorkovsky, Y. Prior, and I. Sh. Averbukh, New J. Phys. **11**, 105039 (2009).

[34] A. G. York, Opt. Express **17**, 13671 (2009).

[35] K. Kitano, H. Hasegawa, and Y. Ohshima, Phys. Rev. Lett. **103**, 223002 (2009).

[36] D. P. Pullman, B. Friedrich, and D. R. Herschbach, J. Chem. Phys. **93**, 3224 (1990).

[37] M. D. Barry, N. P. Johnson, and P. A. Gorry, J. Phys. E **19**, 815 (1986).

[38] I. Sh. Averbukh and N. F. Perelman, Phys. Lett. A **139**, 449 (1989).

[39] R. W. Robinett, Phys. Rep. **392**, 1 (2004).

[40] G. O. Sitz, A. C. Kummel, R. N. Zare, and J. C. Tully, J. Chem. Phys. **89**, 2572 (1988).